*Materials Science Forum Vols. 235-238 (1997) pp. 85-90*
*online at http://www.scientific.net*


# MECHANICAL ALLOYING OF Ni-Nb ALLOYS

M. H. Enayati[1], I. T. H. Chang[2], P. Schumacher[1] and B. Cantor[1]
[1)]*Oxford Centre for Advanced Materials and Composites,Department of Materials, University of Oxford, Parks Road, Oxford OX1 3PH, UK*
[2)]*School of Metallurgy & Materials, University of Birmingham, Birmingham B15 2TT, UK*

**Keywords**: mechanical alloying, ball milling, Ni-Nb alloys, amorphous, nanocrystalline, thermal stability, X-ray diffraction, differential scanning calorimetry

**Abstract**
Elemental Ni-Nb powder mixtures containing 20, 40 and 60 at.% Nb were mechanically alloyed in a centrifugal ball mill. The structural changes in the powders were investigated by X-ray diffractometry, scanning electron microscopy and differential scanning calorimetry as a function of milling time, and were compared to corresponding melt spun materials. The broadening of Nb diffraction peaks with milling time was greater than that of Ni because of a faster accumulation of lattice defects. Mechanical alloying eventually led to a fully amorphous structure but the amorphization reaction was hindered in the presence of methanol acting as a surfactant.

## 1. Introduction

Studies of processing techniques which increase the range of obtainable microstructures and lead to improvements in properties are important for the development of new materials. Mechanical alloying (MA) is a solid-state processing route which involves the dry-milling of powders in a high energy mill [1]. Severe plastic deformation, repeated cold welding and fracturing of powder particles, creation of a high density of lattice defects, and material transfer by diffusion of components during milling provide the means to synthesize materials with very fine microstructures and non-equilibrium phases [2]. The resulting MA powders can subsequently be consolidated by standard powder metallurgy techniques into bulk materials with desirable properties [3].

One of the interesting features of MA is the ability to produce nanocrystalline and amorphous materials. It has been shown that a nano-sized grain structure can be obtained in most materials after sufficient milling time [4-8], often with transformation to an amorphous phase after longer milling times. A great number of alloys such as Ni-Zr [9,10], Ni-Ti [11], Al-Ti [12-14], Fe-Si-B [15] and Al-Ti-Fe [16] have been amorphized by MA. However, there are few reports on the Ni-Nb system [17-19].

The objective of the present work was to study the nanocrystallization and amorphization of some Ni-Nb alloys induced by MA. The structures obtained by MA were compared with those obtained by melt spinning.

## 2. Experimental Techniques

Powder mixtures of elemental Ni (≤300 mesh, 99.9% purity) and Nb (≤325 mesh, 99.8% purity) containing 20, 40, and 60 at.% Nb were mechanically alloyed, nominally at room temperature using a laboratory Fritscl Pulverisette 6 centrifugal mill in an Ar atmosphere with a ball-to-powder weight ratio of ~10:1.Various amounts of methanol as a surfactant were added to a typical powder charge of 17 g prior to MA. For comparison purposes, ribbons of $Ni_{60}Nb_{40}$ were made by melt-spinning on a Cu wheel, with a surface speed of 47 m/s, in inert Ar atmosphere. MA and melt spun samples were characterized by: X-ray diffraction (XRD) in a Philips PW 1729 diffractometer using filtered CuKα radiation (λ=0.1542 nm); scanning electron microscopy (SEM) in a Philips 501 SEM; and differential scanning calorimetry (DSC) in a TA 2200 thermal analyser fitted with a 2010 DSC module using a constant heating rate of 10 K/min from 200 to 670 °C.

**3. Results and Discussion**

*3.1 Structural Changes*

Figure 1 shows XRD traces for $Ni_{60}Nb_{40}$ powders as received and after different MA times. During MA the sharp crystalline diffraction peaks of the as received powder broaden progressively with increasing processing time.

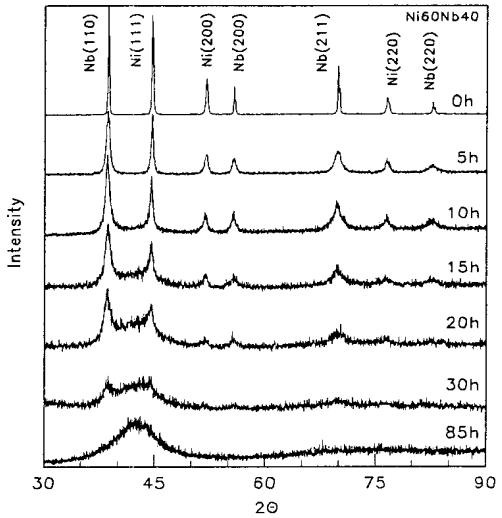


Fig. 1 XRD spectra from $Ni_{60}Nb_{40}$ powder as received and after different MA times.

The broadening of the Ni(111) and Nb(110) diffraction peaks as a function of milling time are compared in Figure 2 by plotting the relative half-peak widths $(W_t-W_0)/W_0$, where $W_0$ and $W_t$ are the diffraction peak width at half-maximum intensity for as received and milled powders respectively. The Nb(110) peak broadens more rapidly than the Ni(111) peak, indicating faster grain size refinement and accumulation of internal strain in the Nb powder. Grain size and internal strain are both determined by a balance between the creation of lattice defects due to intensive plastic deformation, and the annihilation of lattice defects by diffusive annealing which scales with the melting point [4,20,21]. The higher melting point, Nb powder can therefore develop a smaller grain size with greater internal strain, leading to broader diffraction peaks at each milling time. Scherrer's equation gives the grain size $D = 0.91\lambda/W\cos\theta$, where $\lambda$ is the CuK$\alpha$ wave length, W is the diffraction peak width at half-maximum intensity and $\theta$ is the Bragg diffraction angle. After 25 h MA, the values of D calculated from Ni (111) and Nb (110) are 3.5 nm and 2.5 nm respectively. These results disagree with Koch et al. who reported that Ni reaches a smaller grain size than Nb during MA of $Ni_{60}Nb_{40}$ [17].

The progress of amorphization can also be followed from Figure 1. During MA a diffuse amorphous halo develops and grows gradually with increasing processing time, until a fully amorphous structure is formed after 85 h MA. The $Ni_{80}Nb_{20}$ and $Ni_{40}Nb_{60}$ compositions exhibit similar trends during MA, with times to form a fully amorphous structure of 80 and 95 h respectively. In other words the amorphization time increases with increasing Nb content. The position of the diffuse amorphous halo is $2\theta = 44.2°$ for $Ni_{80}Nb_{20}$, and shifts to lower angles with increasing Nb content. The amorphous XRD traces after long MA times were essentially identical to XRD traces from melt spun samples of the same composition.

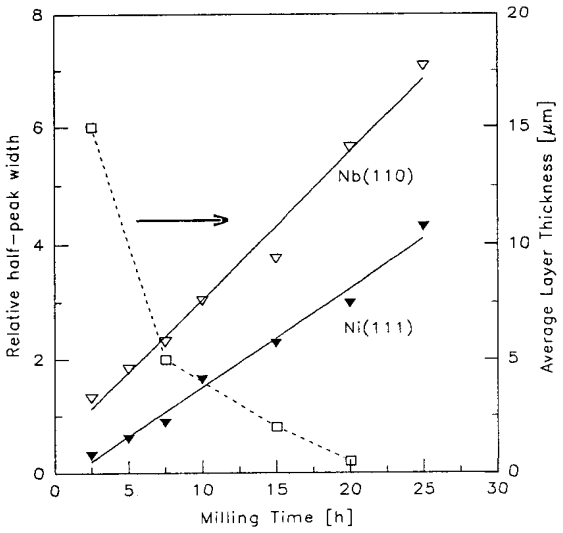


Fig. 2 Relative half-peak width of Ni(111) and Nb(110) peaks (solid lines) and the average layer thickness (dashed line) as a function of MA time for $Ni_{60}Nb_{40}$.

The crystalline diffraction peaks do not shift during MA even at longer times, indicating that no significant alloying takes place and that no intermediate crystalline phase forms as a precursor to the amorphous phase.

Figure 3 shows cross-sectional SEM images of $Ni_{60}Nb_{40}$ powder particles after 2.5 and 7.5 h MA. The MA process produces a coarse layered microstructure consisting of cold welded Ni and Nb layers, with a progressively refined layer thickness with increasing MA processing time. As shown in Figure 2 the layer thickness decreases proportional to the grain size within the layers, and both contribute to the broadening of the X-ray diffraction peaks shown in Figure 2. The microstructures of fully amorphized powders were featureless in the SEM.

*3.2 Influence of Methanol*

Agglomeration of the powders on the pot and ball surfaces is a problem with MA processing, which is commonly overcome by adding a liquid surfactant such as methanol to the powder mixture [22,23]. Figure 4 shows XRD spectra from $Ni_{60}Nb_{40}$ powder as received and after 40 h MA, with 0, 0.5 and 2 ml of methanol added to the powder mixture prior to MA. The fraction of residual crystalline phase estimated from the intensity of the crystalline peaks increases with increasing amount of methanol. With 2 ml methanol no fully amorphous samples were obtained; whereas without methanol for the same milling time, a fully amorphous structure was readily obtained. Cold welding and therefore interdiffusion of elements along Ni/Nb interfaces appear to be hindered by methanol, which therefore effectively retards the amorphization reaction. The milling of Ni-Nb powder mixtures as well as elemental Nb powders in the presence of methanol results in the displacement of Nb peaks towards lower angles. The shift for the Nb(110) peak is 1.18° which shows that the Nb lattice is considerably expanded. This behaviour has not been reported previously [22-23] and its explanation is not yet clear.

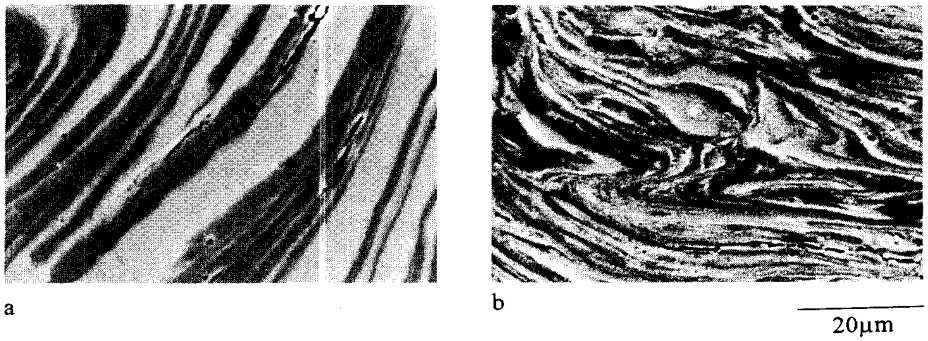


Fig. 3 Cross-sectional SEM images of $Ni_{60}Nb_{40}$ powder particles after (a) 2.5 and (b) 7.5 h MA.

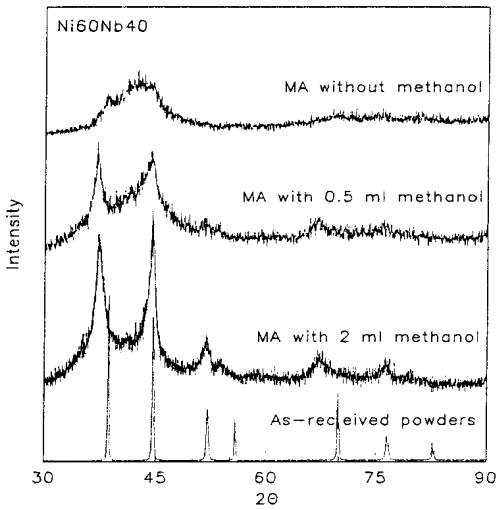


Fig. 4 XRD spectra from of $Ni_{60}Nb_{40}$ as received powder and after 40 h MA with different amounts of methanol.

3.3 *Thermal Behaviour*

Figure 5 shows DSC traces from $Ni_{60}Nb_{40}$ as received powder and after different milling times. After 10-30 h MA, the DSC traces show a small, broad exotherm around 530 °C. This exotherm is caused by the reaction of Ni and Nb in the multilayered structure to form crystalline intermetallic compounds. The reaction process is aided by the extensive Ni/Nb interfaces which facilitate Ni/Nb interdiffusion during heating. As MA proceeds to 50-85 h milling, the fraction of crystalline intermetallic phases formed during heating decreases, and the broad 530 °C peak disappears. Instead, a sharp exothermic peak develops gradually corresponding to crystallization of the amorphous phase

with onset and peak crystallization temperatures ($T_0$ and $T_p$) of 646° and 663 °C respectively. $T_0$ as well as $T_p$ are not influenced significantly by milling time, indicating that the crystallization process is independent of the presence of crystalline intermetallic phases in partially amorphized powders. In MA samples, it is likely that there are always large numbers of heterogeneous crystalline nuclei, which remain from incomplete milling, so that the crystallization kinetics are always dominated by crystal growth. The DSC trace from melt spun $Ni_{60}Nb_{40}$ is similar to MA $Ni_{60}Nb_{40}$, with similar $T_0$ and $T_p$ values of 645 and 658 °C respectively. Table 1 lists the $T_0$ and $T_p$ values for the different MA alloys, showing that $Ni_{60}Nb_{40}$ is the most stable amorphous alloy.

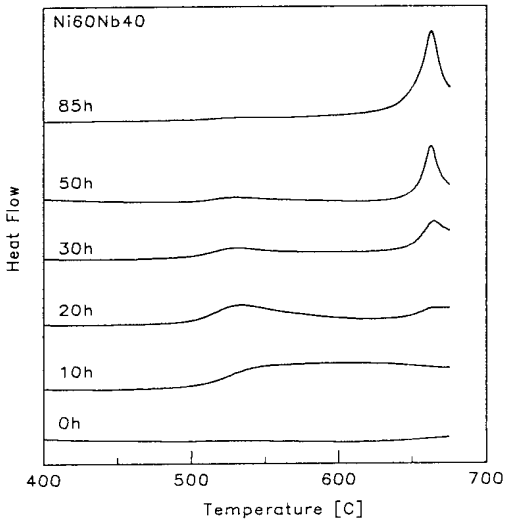


Fig. 5 DSC traces from $Ni_{60}Nb_{40}$ powder as received and after different MA times.

Table 1 Onset temperature ($T_0$) and crystallization temperature ($T_p$) of three Ni-Nb amorphous alloys prepared by MA

| Composition | $T_0$[°C] | $T_p$[°C] |
|---|---|---|
| $Ni_{80}Nb_{20}$ | 486 | 498 |
| $Ni_{60}Nb_{40}$ | 646 | 663 |
| $Ni_{40}Nb_{60}$ | 628 | 639 |

## 4. Conclusions

Elemental Ni-Nb powder mixtures containing 20, 40 and 60 at.% Nb were mechanically alloyed in a centrifugal ball mill. The structural changes in the powders were investigated by XRD, SEM and DSC as a function of milling time, and were compared to corresponding melt spun materials. The broadening of Nb diffraction peaks with milling time was greater than that of Ni because of a faster accumulation of lattice defects. Mechanical alloying eventually led to a fully amorphous structure but the amorphization reaction was hindered in the presence of methanol acting as a surfactant. It was shown that the $Ni_{60}Nb_{40}$ amorphous alloy is the most stable composition on heat treatment. Moreover, the presence of crystalline phases in partially amorphized powder did not influence the thermal stability of the amorphous phase. The XRD and DSC traces of MA and melt spun $Ni_{60}Nb_{40}$ samples were found to be quite similar.

**Acknowledgments**

We would like to thank the Ministry of Culture and Higher Education of Iran and the UK Engineering and Physical Science Research Council for financial support.

**References**

[1] J. S. Benjamin, Metall. Trans. **1**, 2943 (1970).
[2] C. C. Koch, Annu. Rev. Mater. Sci. **19**, 121 (1989).
[3] L. He and E. Ma, J. Mater. Res. **11**, 72 (1996).
[4] J. Eckert, J. C. Holzer, C. E. Kril III and W. L. Johnson, J. Mater. Res. **7**, 1751 (1992).
[5] E. Hellstern, H. J. Fechet, Z. Fu and W. L. Johnson, J. Appl. Phys. **65**, 305 (1989).
[6] T. D. Shen, C. C. Koch, T. L. Mccormick, R. J. Nemanich, J. Y. Huang and J. G. Huang, J. Mater. Res. **10**, 139 (1995).
[7] H. J. Fechet, E. Hellstern, Z. Fu and W. L. Johnson, Adv. Powder Metall. **1**, 111 (1989).
[8] H. J. Fechet, E. Hellstern, Z. Fu and W. L. Johnson, Metall. Trans. **A 21**, 2333 (1990).
[9] Y. Chen, M. Bibole, R. Le Hazif and G. Martin, Phys. Rev. **B 48**, 14 (1993).
[10] F. Petzoldt, J. Less-Com. Met. **140**, 85 (1988).
[11] D. Z. Sun, L. Z. Cheng, Y. M. Zhang and K. Yuang Ho, J. Alloys and Compounds **186**, 33 (1992).
[12] E. Bonetti, G. Cocco, S. Enzo and G. Valdre, Mater. Sci. Techn. **6**, 1258 (1990).
[13] G. Cocco, I. Soletta, L. Battezzati, M. Bariccoands and S. Enzo, Phil. Mag. **B 61**, 473 (1990).
[14] W. Guo, S. Martelli, N. Burgio, M. Magini, F. Padella and E. Paradiso, J. Mater. Sci. **26**, 6190 (1990).
[15] M. X. Quan, K. Y. Wang, T. D. Shen and J. T. Wang, J. Alloys and Compounds **194**, 325 (1993).
[16] S. Saji, Y. Neishi, H. Araki, Y. Minamino and T. Yamane, Metall. Mater. Trans. **A 26**, 1305 (1995).
[17] C. C. Koch, O. B. Cavin, C. G. Mckamey and J. O. Scarbrough, Appl. Phys. Lett. **43**, 1017 (1983).
[18] F. Petzoldt, B. Scholz and H. D. Kunze, Mater. Lett. **5**, 280 (1987).
[19] F. Petzoldt, B. Scholz and H. D. Kunze, Mater. Sci. Eng. **97**, 25 (1988).
[20] C. C. Koch, Nanostructured Materials **2**, 109 (1993).
[21] A. Benghalem and D. G. Morris, Acta Metall. Mater. **42**, 4071 (1994).
[22] G. H. Chen, C. Suryanarayana and F. H. Froes, Metall. Mater. Trans. **A 26**, 1379 (1995).
[23] M. Zdujic, D. Sakala, L. Karanovic, M. Krstanovic, K. F. Kobayashi and P. H. Shingu, Mater. Sci. Eng. **A 161**, 237 (1993).